AGU PUBLICATIONS

Geophysical Research Letters

RESEARCH LETTER
10.1002/2017GL075860

Key Points:
- Mean global permeability is higher with detailed unconsolidated mapping
- Representative permeability values are applied to a new global map to produce first geologically constrained, two-layer global map of shallower and deeper permeability
- Maps are crucial for next generation of land surface, hydrologic, and climate models

Supporting Information:
- Supporting Information S1

Correspondence to:
T. Gleeson,
tgleeson@uvic.ca

Citation:
Huscroft, J., Gleeson, T., Hartmann, J., & Börker, J. (2018). Compiling and mapping global permeability of the unconsolidated and consolidated Earth: GLobal HYdrogeology MaPS 2.0 (GLHYMPS 2.0). *Geophysical Research Letters*, *45*, 1897–1904. https://doi.org/10.1002/2017GL075860

Received 6 OCT 2017
Accepted 26 JAN 2018
Accepted article online 12 FEB 2018
Published online 28 FEB 2018

Compiling and Mapping Global Permeability of the Unconsolidated and Consolidated Earth: GLobal HYdrogeology MaPS 2.0 (GLHYMPS 2.0)

Jordan Huscroft[1,2], Tom Gleeson[2], Jens Hartmann[3], and Janine Börker[3]

[1]Bioresource Engineering, McGill University, Montreal, Quebec, Canada, [2]Department of Civil Engineering and School of Earth and Ocean Sciences, University of Victoria, Victoria, British Columbia, Canada, [3]Institute for Geology, Center for Earth System Research and Sustainability, Universität Hamburg, Hamburg, Germany

Abstract The spatial distribution of subsurface parameters such as permeability are increasingly relevant for regional to global climate, land surface, and hydrologic models that are integrating groundwater dynamics and interactions. Despite the large fraction of unconsolidated sediments on Earth's surface with a wide range of permeability values, current global, high-resolution permeability maps distinguish solely fine-grained and coarse-grained unconsolidated sediments. Representative permeability values are derived for a wide variety of unconsolidated sediments and applied to a new global map of unconsolidated sediments to produce the first geologically constrained, two-layer global map of shallower and deeper permeability. The new mean logarithmic permeability of the Earth's surface is -12.7 ± 1.7 m^2 being 1 order of magnitude higher than that derived from previous maps, which is consistent with the dominance of the coarser sediments. The new data set will benefit a variety of scientific applications including the next generation of climate, land surface, and hydrology models at regional to global scales.

1. Introduction

Permeability, the ability of a porous material to transmit fluids, is fundamental in controlling the rate in which fluids flow in the surface of the Earth, which impacts a wide variety of shallow and deep Earth processes and water resource evaluation (Achtziger-Zupančič et al., 2017; Fan, 2015; Fan et al., 2015; Gleeson & Ingebritsen, 2016; Ingebritsen & Manning, 1999). The lack of regional permeability data in the past has hampered integration of groundwater dynamics and interactions into regional to global land surface and hydrology models (Bierkens, 2015; Fan, 2015). Recently, permeability was compiled for major rock types and paired with lithology maps in the GLobal HYdrogeology MaPS or GLHYMPS (Gleeson et al., 2014, 2011). GLHYMPS permeability and porosity maps have been implemented in several regional to global land surface and hydrology models (Bierkens, 2015; de Graaf et al., 2014; Gleeson et al., 2016; Leibowitz et al., 2016; Maxwell et al., 2016, 2015; Maxwell & Condon, 2016; Milly et al., 2014; Sutanudjaja et al., 2014; Xu & Liu, 2017). But the current global, high-resolution permeability maps only separate unconsolidated materials into fine-grained and coarse-grained, which is problematic because (1) unconsolidated sediments have a wide range of permeability values from highly permeable sands to very low permeability clays and (2) unconsolidated sediments cover significant portions of the Earth. Quantifying the permeability of unconsolidated materials is challenging due to the inherent variation, heterogeneity, and mixing in grain sizes in many depositional environments. Consequently, the permeability of various unconsolidated grain sizes and sediment types have not been robustly quantified, especially at larger scales.

The objective of this paper is to derive representative permeability values for different types of unconsolidated sediments and apply these representative permeability values to a new global map of unconsolidated sediments to produce a global, two-layer map of shallower and deeper permeability based on geological mapping for the first time (GLHYMPS 2.0). This study improves upon existing GLHYMPS data sets by better representing unconsolidated sediments and taking advantage of recent advances in mapping unconsolidated sediments in the Global Unconsolidated Map (GUM) (Börker et al., 2018) and depth to bedrock in SoilGrids (Shangguan et al., 2017). The improved resolution and refinement of global maps allow for enhanced unconsolidated permeability classifications, which we quantify using an expanded and refined permeability data compilation. Based on GLHYMPS, de Graaf et al. (2017) developed a two-layer global groundwater model that estimated aquifer thickness, and thus transmissivity, and stochastically

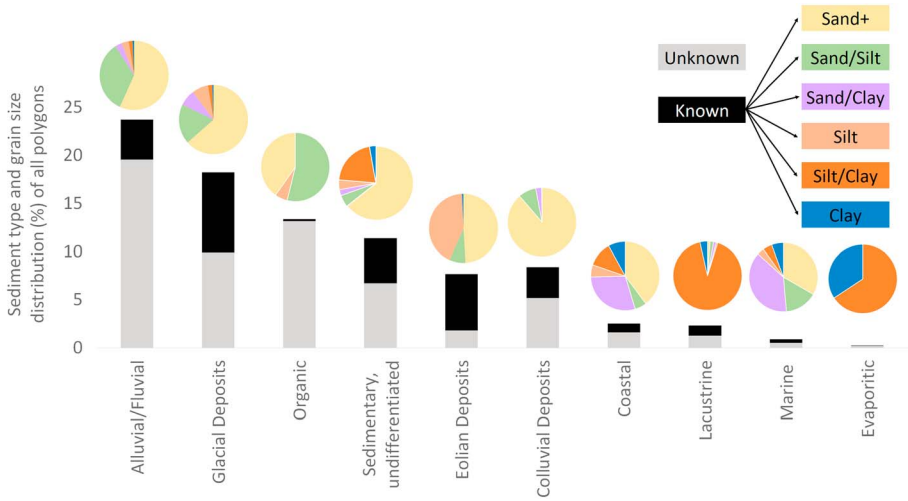

Figure 1. Histogram of different sediment types and pie charts of grain size distributions in each sediment type. The colored pie charts represent the most common occurring grain sizes for each general sediment group, while the black and grey bars on the histogram represent known and unknown (including mixed) percentages of grain sizes.

represented the likelihood of a confining layer. We improve significantly on this two-layer representation by having two separate sources of geological data, rather than stochastically representing the likelihood of a confining layer. The new two-layer permeability product will enable the simulation of deeper groundwater flow processes with longer, slower flow paths and confined aquifer conditions, as well as refine our understanding of unconsolidated sediments in Earth processes.

2. Analysis of the Global Unconsolidated Map (GUM)

The original GLHYMPS (Gleeson et al., 2014) were developed by pairing permeability data and the Global Lithological Map (GLiM) (Hartmann & Moosdorf, 2012). One of the major limitations of the GLiM was the lack of detailed refinement of unconsolidated sediment types, leading to greater uncertainty of individual polygons, and in some regions, the absence of surface sediments overlying the deeper lithological units (Hartmann & Moosdorf, 2012). To address this concern, the GUM was recently developed, synthesizing global, near-surface, digital lithology mapping (Börker et al., 2018). The unconsolidated units of GLiM had an average polygon size of 123 km^2, with a global coverage of 4.58×10^7 km^2, while the new GUM has an average polygon size of 91.2 km^2 with a global coverage of 8.14×10^7 km^2. The new unconsolidated map has a 23.6% increase in global unconsolidated sediment land area coverage. Remaining uncovered land area not included in GUM is due to a lack of accessible unconsolidated data or the exclusion of mapped consolidated surface sediments. The GUM database records sediment type (e.g., coastal) and depending on data availability, sediment subtype (e.g., marsh sediment subtype within the coastal sediment type) and grain size (e.g., clay). We analyzed the global spatial distribution and frequency of sediment types, sediment subtypes, and grain size to develop a permeability classification system that is consistent with the new GUM.

Figure 1 shows the sediment classes, grain size distributions, and distribution of corresponding known and unknown or mixed grain sizes for 870,668 individual polygons covering an area of 8.14×10^7 km^2. The GUM is composed of 10 sediment types (excluding water, ice, man-made, and pyroclastic as seen in Figure 1), which are further refined into 25 sediment subtypes (Table S1). Polygons without detailed descriptions are classified as undifferentiated sediment types rather than refined to a sediment subtype. Alluvial/fluvial is the dominant sediment type with over 23% of GUM polygons with an area of 1.5×10^7 km^2 or 19% of all GUM land coverage.

Wherever possible sediment grain size is mapped for GUM polygons as one of six grain sizes: sand and coarser (herein called sand+), sand/silt, sand/clay, silt, silt/clay, and clay. The categories with two grain sizes (e.g., sand/silt) do not infer a predominance of one grain size or another. Analysis of GUM data revealed that 68% of the polygons (representing 78% of land surfaces mapped) do not have grain size information attached. Large percentages of polygons of various sediment types were coupled with unknown or mixed

grain size information, and therefore, where grain size information was not available, grain size classification was based on statistical frequency (see section 4).

3. Permeability Compilation

A literature compilation was used to derive representative permeability values for the GUM polygons considering sediment types, sediment subtypes or grain sizes. Generally, there are three readily available sources of permeability data: textbooks, field data from hydraulic tests, and calibrated groundwater models. We compiled and compared permeability values from textbooks and calibrated groundwater models but relied on calibrated groundwater models because the methods and uncertainties of their derivation are better documented than textbook values. Canonical permeability values or ranges from textbooks are generally considered a reliable source of information, yet surprisingly, none of the textbooks we examined documented the source of the permeability values. Field data generally represent the small scale ($<$1 m to hundreds of meters), and following Gleeson et al. (2011), we are interested in regional-scale permeability values. Since it is well known that the scale of observation impacts permeability (e.g., Brace, 1980), we do not include point observations (e.g., core or air permeameter derived) or small-scale hydraulic tests (e.g., pump test derived). Therefore, we do not compile or further analyze field data (although calibrated groundwater models often are based on field data from the model domain that is then calibrated to be consistent with water levels or other observations). We explored the possibility of compiling permeability values for the mapped sediment types and subtypes, but most sediment types and subtypes had few or no identified permeability values from calibrated groundwater models. Only for the most common sediment types (alluvial/fluvial, glacial, lacustrine, evaporitic, and sedimentary) had more than six permeability values from calibrated regional-scale groundwater models. Additionally, it is well recognized that most sediment types represent a mixture of grain sizes. Therefore, our permeability compilation focused on grain sizes, which is also consistent with textbook practices. We used a grain size classification system that was consistent with the six grain size categories in GUM and calculated the geometric mean for each grain size category, following Gleeson et al. (2011). Grain size distribution is also known to control permeability (Carrier III, 2003), and a classification system could be based on grain size distribution, although this is not possible since calibrated groundwater models rarely describe the grain size distribution of model units. Instead, we crudely represent grain size distribution with mixed grain size categories (i.e., sand/silt, sand/clay, and silt/clay), which are consistent with textbook and numerical modeling practices.

The compilation process, model criteria, and data reduction process was consistent with methods used by Gleeson et al. (2011) that considered data from models that are calibrated (as reported in the reference), peer-reviewed (academic papers or government reports), regional-scale (minimum lateral scale of 5 km), and shallow (part of a geological unit in the model within 100 m depth of land surface). Thirteen new calibrated groundwater models with unconsolidated permeability data were added to the existing data compilation, which previously included 18 calibrated groundwater models of unconsolidated sediments. The updated database now includes 31 unique groundwater models from 11 countries and includes coverage of over 13 states of the United States of America. Our rigorous model criteria meant that $>$10 articles would be reviewed for each article that met the criteria. Each article that met criteria typically provided numerous hydraulic conductivity values, such that $>$200 individual permeability values for unique unconsolidated materials were extracted from these sources. The large geographic distribution ensures that the compilation incorporates a diverse variety of depositional settings, as well as different approaches to modeling and calibration. A number of sources did not meet the model criteria described above (Table S2).

To determine if the calculated geometric means of compiled, calibrated grain size permeability values were reasonable (Table 1), the results from calibrated groundwater models (Table S4) were compared to ranges from standard textbook values (Table S3). Figure 2 shows that the geometric mean permeability values from calibrated groundwater models are consistently within 1 order of magnitude of the mode of the textbook distributions for each grain size classification. The exception to this occurs in the silt/clay unit, where no textbook values were found.

4. A New Global Two-Layer Permeability Map

The GUM and GLiM are both global maps representing with the near-surface conditions for unconsolidated and all lithologies, respectively. The goal of the global mapping herein is to use these two products to

Table 1
Grain Size, Permeability Value, and Associated Sediment Type of GUM Unconsolidated Sediment Data

Grain size	Permeability log(*k*) geometric mean (m^2)	Permeability log(*k*) standard deviation (m^2)	Sediment type	Sediment subtype	GLHYMPS 2.0 polygon coverage %	GLHYMPS 2.0 land area coverage %
Sand+	−10.52	−1.61	A, C, E, G, U, Y	At, Ed, Gf, Gt, Yb, Yd, Yl, Ys	24.8	29.8
Sand/Silt	−11.94	−1.73	O	Af, Er, Gm, Gp, Op, Or	8.8	2.1
Sand/clay	−11.35	−1.30	M	Al, Ca	4.5	6.0
Silt	−14.13	−1.37		Ea, El	2.1	3.0
Silt/clay	−14.95	−2.55	L, P	Ae, Gl, Pg, Pp, Ps	2.5	2.4
Clay	−15.77	−2.06		Ap, Ym	0.9	0.7

Note. Sediment Type and subtype: A, alluvial/fluvial, Ae, fluvial-eolian, Af, alluvial fan deposits, Al, fluvial-lacustrine, Ap, floodplain deposits, At, alluvial terrace deposits; C, colluvial deposits, Ca, alluvial/Colluvial; E, eolian, Eu, eolian deposits, Ea, loess-like, silt, but not eolian (alluvial/colluvial), Ed, dune sands, El, loess, Er, loess derivative, reworked, mixture; G, glacial deposits, Gf, glacio-fluvial, Gl, glacio-lacustrine, Gm, glacio-marine, Gp, proglacial, Gt, Till; L, lacustrine deposits; M, marine deposits; O, organic deposits, Op, peat, Or, reef; P, evaporitic deposits, Pg, gypsum, Pp, playa deposits, Ps, salt; U, sedimentary, undifferentiated; Y, coastal deposits, Yb, beach deposits, Yd, delta deposits, Yl, lagoonal deposits, Ym, marsh deposits, Ys, swamp deposits.

develop a new two-layer map of shallower and deeper permeability that can be used in regional- to global-scale land surface and hydrology models. GUM only covers 55% global land surface so the GUM data set alone is not sufficient to create a new map with global coverage. Additionally, 68% of GUM polygons lack grain size information (Figure 1) so although it is generally recognized that grain size controls permeability in unconsolidated materials, it was not possible to directly pair permeability values with polygons solely using grain size. For the polygons without grain size information, we paired the permeability of the dominant reported grain size (ranked by frequency of polygons) of each sediment type and sediment subtype (Table 1) with the permeability value of the grain size (Figure 2). We considered calculating a composite permeability value for sediment types and subtypes based on the percentages of grain sizes in each category but found that this is a meaningless and artificial calculation using spatial distributions (% polygons with certain grain size) to calculate a composite permeability of mixed grain sizes. Given the data available, the assumption that the dominant grain size (Figure 1) is indicative of the permeability of sediment types and subtypes seems more appropriate.

We developed a framework for pairing permeability values with mapped polygons (Figure 3) based on certainty of source data to pair permeability data with mapped GUM polygons for the shallower layer of the two-layer map. First, if the area was not mapped in GUM, permeability was assigned directly from GLHYMPS. Second, for the polygons in GUM with grain size information, the grain size was used to pair with permeability values for each grain size. Third, for the polygons with sediment subtype information, the

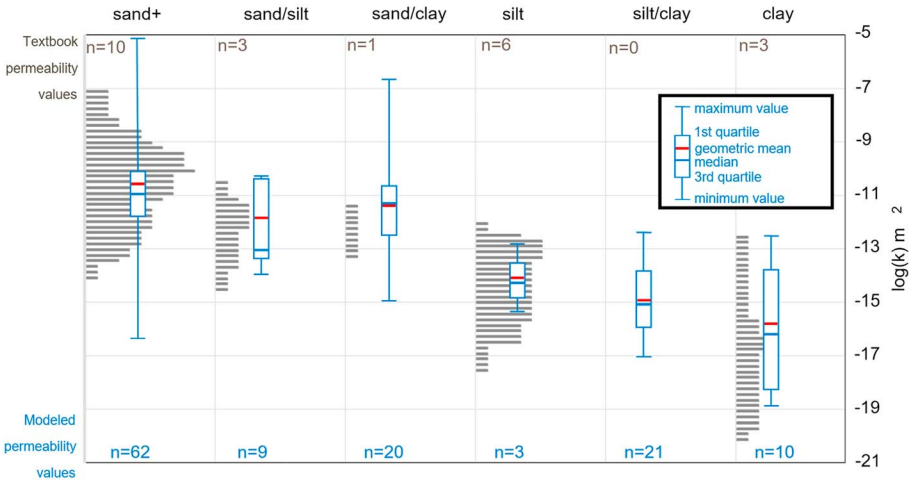

Figure 2. The permeability of different grain sizes comparing textbook values (grey histograms, with textbook ranges divided over discrete bins and summed as a frequency histogram) with calibrated model values (blue box plots). The frequency for each data type and grain size category is shown.

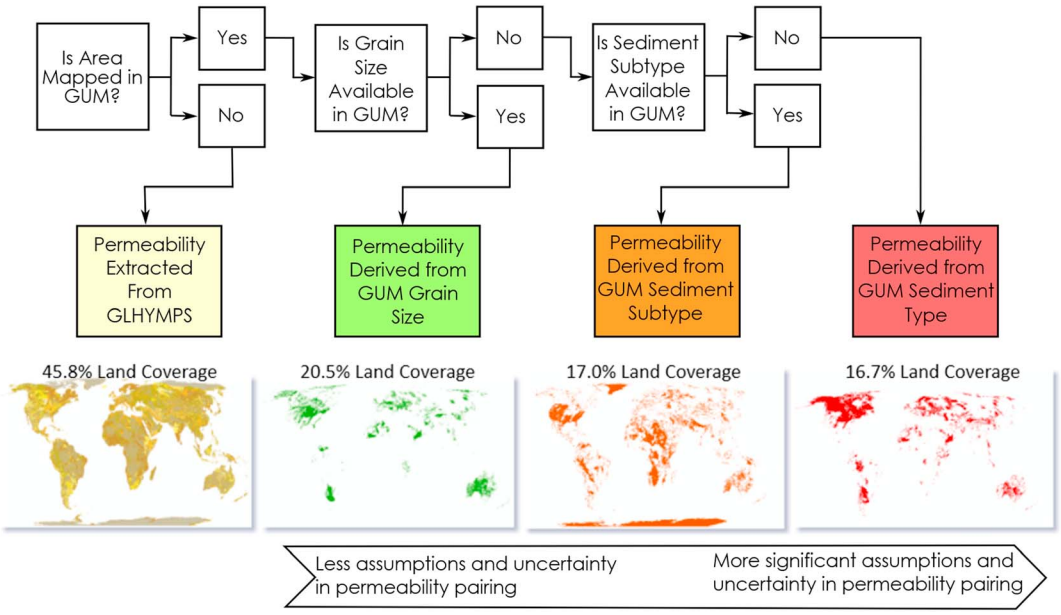

Figure 3. Logic and workflow for deriving permeability values of shallower layer, based on the degree of assumptions and levels of uncertainty.

permeability for the sediment subtype (based on the permeability of the dominant grain size as described above) was applied. Finally, for the polygons without sediment subtype information, the permeability of the sediment type was similarly applied.

Figure 4 outlines the three components that together form GLHYMPS2.0. To clarify the depth of the shallower layer, the mean depth to bedrock from Shangguan et al. (2017) was calculated and mapped for each GUM polygon. The deeper layer, the original GLHYMPS map, was derived from the GLiM. The depth of the deeper layer is considered to be on the order of ~100 m, following Gleeson et al. (2011); however, clarifying, reporting, or calculating a precise depth is not possible. All permeabilities are expected to decrease with depth below the deeper layer.

Following the process outlined in Gleeson et al. (2014), global permafrost (Gruber, 2012) was included as a secondary permeability parameter. In areas of continuous permafrost (defined at PZI $>$ 0.99), two values of permeability are given, one representative of permafrost with $\log(k) = -20$ m^2 and the other with the value of the calculated surficial material or value assigned in GLHYMPS. The spatial extent of the permafrost zone is identical to GLHYMPS; however, its impact on unconsolidated sediment is now updated.

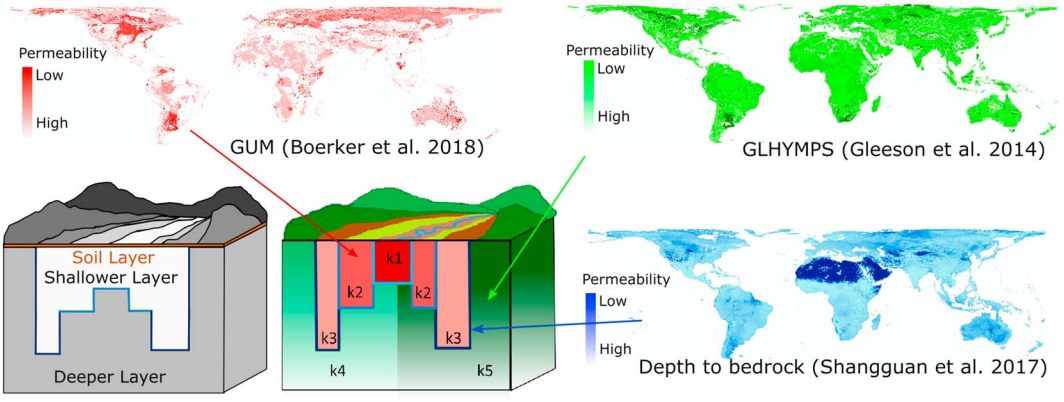

Figure 4. The structure of GLobal HYdrogeology MaPS 2.0. Surficial materials representative of Global Unconsolidated Map (GUM, red), near-surface materials taken from GLobal HYdrogeology MaPS outside of GUM coverage areas (green), and GUM surface layer thickness taken from SoilGrids depth to bedrock map in (blue).

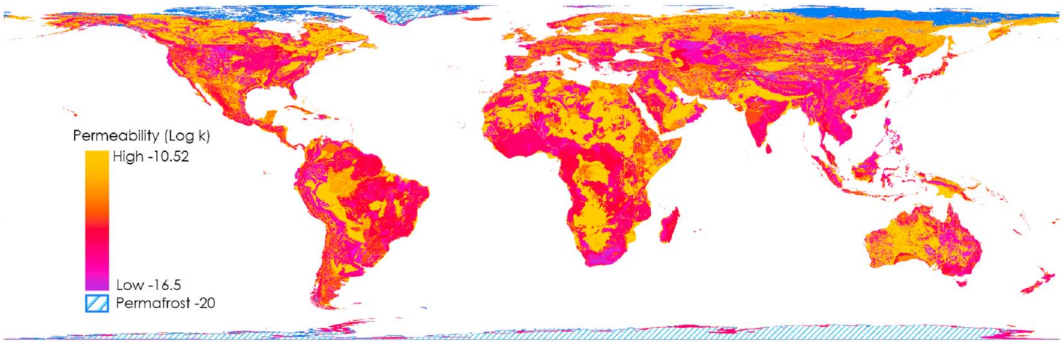

Figure 5. New representation of high-resolution surficial unconsolidated sediments and associated global permeability, GLobal HYdrogeology MaPS 2.0. Permafrost areas included and with assumed log(k) = −20.

The results of the synthesis of mapped sediment types, permeability values compilation, permafrost extent, and retained GLHYMPS values are presented in Figure 5 showing the new global distribution of permeability values. Additionally, Table 1 includes the distribution permeability values for each sediment type and subtype. The spatially distributed mean logarithmic permeability for land surfaces is -12.7 ± 1.7 m^2 without permafrost or -13.0 m^2 with permafrost. These global averages are higher than the results of GLHYMPS by 1 order of magnitude, which is consistent with the dominance of the coarse sediment group (sand+), representing 29.8% of GUM land area coverage.

A new estimation of the distribution and mean of global transmissivity can be calculated as the product of the depth to bedrock and the unconsolidated permeability. Previously, de Graaf et al. (2014) calculated global transmissivity based on an algorithm of sediment thickness and the permeability data from GLHYMPS. Our new data set allows a more geologically grounded calculation of the distributions of transmissivity of the shallower layer for specific regions since a robust estimate of depth to bedrock is used as well as the refined two-layer permeability database. Since bedrock permeabilities are expected to decrease with depth below the deeper layer, assigning a precise thickness (beyond the approximation of ~100 m) is meaningless. For this reason, we do not calculate a transmissivity of the deeper layer.

5. Applications and Limitations

The absence of a compilation of high resolution unconsolidated sediment maps of global coverage has limited the global investigation of detailed hydrogeological processes. With the introduction of GUM, leading to the development of GLHYMPS 2.0, the availability of a global map of both unconsolidated sediments and now globally distributed permeability, the possibility of investigating more complex problems, such as the sensitivity of shallow aquifers to human extraction or the impacts of climate-change on regional unconsolidated aquifer recharge, is possible. The applications of these permeability findings in their current form are expected to be invaluable in the improvement of regional to global climate, land surface and hydrology models, assessments of continental groundwater supply, and providing preliminary tools to help evaluate areas where water scarcity risk is a concern. Due to the integration of multiple data sources (GUM, GLiM, GLHYMPS, and SoilGrids), and the assumptions required to complete a global data set (continuous permafrost coverage, saturated permeability values, etc.), a number of limitations have been identified that reduce the certainty of the results. A number of artifacts were present in both the GLiM and GUM, which are a result of a combination of the varied mapping methods and subjectivity in interpreting data, nonunique mapping standards considering the various geological data sources, and the use of low-resolution maps when access to high-resolution coverage was not available. These artifacts have resulted in abrupt changes in mapped units over short distances, especially across provincial/state and international boundaries, and were further compounded through the merging of the two maps (GUM and GLiM). The only way to eliminate these artifacts at political boundaries is a global effort to consistently re-map such as Federal Institute for Geosciences and Natural Resources/United Nations Educational, Scientific and Cultural Organization (2008) and Dürr et al. (2005), which were conducted at much coarser resolutions. Global re-mapping at high resolution is beyond the scope of this research.

As GUM was created through the compilation of numerous maps of varying resolution, full global coverage was not obtained due to the inaccessibility of maps from certain nations, and by the presence of outcropping bedrock formations. Additionally, grain size information for large areas of the world were either absent, or general classifications were applied to large areas. Permeability was assigned to GUM polygons based on the distribution of grain sizes and sediment types according to the GUM database. Until complete global grain size coverage (ideally with grain size distribution) is available, assumptions like this have to be made.

The final recognized limitation is the highly simplified classification system that does not differentiate between percentages of mixtures (i.e., a sandy clay and a clay sand would both be classified as a sand/clay). This level of simplification was consistent with the globally available unconsolidated mapping and the limited possibility of differentiating more unique grain size values. Building upon the calibrated permeability data set size and classifying grain sizes distributions as they were identified in literature may allow for novel methods of matching grain size to sediment types. Further work may use local- to regional-scale knowledge on the facies of sediment types to improve grain size information, but this is outside the scope of this work.

6. Conclusion

The lack of globally continuous unconsolidated permeability data has been a limiting factor in the development of more complex hydrological models in the past due. The development of GUM, coupled with our data set of compiled calibrated groundwater permeability values, and supplemented by GLHYMPS permeability values for areas without mapped or nonexistent unconsolidated sediments, resulted in the assemblage of a new global surface permeability map, GLHYMPS2.0. We have mapped permeability across all land surfaces and found a new average global permeability of -12.7 ± 1.7 m^2, or -13.0 m^2 when including permafrost areas. We are confident that this new global permeability estimation, through the inclusion of shallower unconsolidated materials (GUM), is a more realistic approximation compared to the previous GLHYMPS permeability (Gleeson et al., 2014). This new data set is expected to benefit a variety of scientific applications in the next generation of regional to global hydrologic, land surface, and climate models.

Acknowledgments
The full data set will be available upon publication through the University of Victoria dataverse, figshare and CUAHSI in vector format so it can be analyzed or gridded at any desired resolution. The work was funded by the National Science and Engineering Research Council and German Science Foundation (DFG) through the Cluster of Excellence CLISAP2 (DFG Exec177, Universität Hamburg) and PALMOD project BMBF-project PALMOD (Ref 01LP1506C) through the German Ministry of Education and Science (BMBF) as Research for Sustainability initiative (FONA). The authors do have any conflict of interest.

References

Achtziger-Zupančič, P., Loew, S., & Mariéthoz, G. (2017). A new global database to improve predictions of permeability distribution in crystalline rocks at site scale. *Journal of Geophysical Research: Solid Earth*, *122*, 3513–3539. https://doi.org/10.1002/2017JB014106

Bierkens, M. F. P. (2015). Global hydrology 2015: State, trends, and directions. *Water Resources Research*, *51*, 4923–4947. https://doi.org/10.1002/2015WR017173

Börker, J., Hartmann, J., Romero-Mujalli, G., & Amann, T. (2018). Terrestrial sediments of the Earth: Development of a Global Unconsolidated Sediments Map data base (GUM). *Geochemistry, Geophysics, Geosystems*. https://doi.org/10.1002/2017GC007273

Brace, W. F. (1980). Permeability of crystalline and argillaceous rocks. *International Journal of Rock Mechanics and Mining Science and Geomechanics Abstracts*, *17*(5), 241–251. https://doi.org/10.1016/0148-9062(80)90807-4

Carrier, W. D. III (2003). Goodbye, hazen; hello, kozeny-carman. *Journal of Geotechnical and Geoenviromental Engineering*, *129*(11), 1054–1056. https://doi.org/10.1061/(ASCE)1090-0241(2003)129:11(1054)

de Graaf, I. E. M., Sutanudjaja, E. H., van Beek, L. P. H., & Bierkens, M. F. P. (2014). A high resolution global scale groundwater model. *Hydrology and Earth System Sciences Discussions*, *11*(5), 5217–5250. https://doi.org/10.5194/hessd-11-5217-2014

de Graaf, I. E. M., van Beek, R. L. P. H., Gleeson, T., Moosdorf, N., Schmitz, O., Sutanudjaja, E. H., & Bierkens, M. F. P. (2017). A global-scale two-layer transient groundwater model: Development and application to groundwater depletion. *Advances in Water Resources*, *102*, 53–67.

Dürr, H. H., Meybeck, M., & Dürr, S. H. (2005). Lithologic composition of the Earth's continental surfaces derived from a new digital map emphasizing riverine material transfer. *Global Biogeochemical Cycles*, *19*, GB4S10. https://doi.org/10.1029/2005GB002515

Fan, Y. (2015). Groundwater in the Earth's critical zone: Relevance to large-scale patterns and processes. *Water Resources Research*, *51*, 3052–3069. https://doi.org/10.1002/2015WR017037

Fan, Y., Richard, S., Bristol, R. S., Peters, S. E., Ingebritsen, S. E., Moosdorf, N., et al. (2015). DigitalCrust—A 4D data system of material properties for transforming research on crustal fluid flow. *Geofluids*, *15*(1-2), 372–379. https://doi.org/10.1111/gfl.12114

Federal Institute for Geosciences and Natural Resources/United Nations Educational, Scientific and Cultural Organization (2008). Groundwater resources of the world 1:25 000 000.

Gleeson, T., Befus, K. M., Jasechko, S., Luijendijk, E., & Cardenas, M. B. (2016). The global volume and distribution of modern groundwater. *Nature Geoscience*, *9*(2), 161–167. https://doi.org/10.1038/ngeo2590

Gleeson, T., & Ingebritsen, S. E. (Eds.) (2016). *Crustal Permeabilty* (pp. 249–259). Chinchester, UK: John Wiley.

Gleeson, T., Moosdorf, N., Hartmann, J., & van Beek, L. P. H. (2014). A glimpse beneath Earth's surface: GLobal HYdrogeology MaPS (GLHYMPS) of permeability and porosity. *Geophysical Research Letters*, *41*, 3891–3898. https://doi.org/10.1002/2014GL059856

Gleeson, T., Smith, L., Moosdorf, N., Hartmann, J., Dürr, H. H., Manning, A. H., et al. (2011). Mapping permeability over the surface of the Earth. *Geophysical Research Letters*, *38*, L02401. https://doi.org/10.1029/2010GL045565

Gruber, S. (2012). Derivation and analysis of a high-resolution estimate of global permafrost zonation. *The Cryosphere*, *6*(1), 221–233. https://doi.org/10.5194/tc-6-221-2012

Hartmann, J., & Moosdorf, N. (2012). The new global lithological map database GLiM: A representation of rock properties at the Earth surface. *Geochemistry, Geophysics, Geosystems*, *13*, Q12004. https://doi.org/10.1029/2012GC004370

Ingebritsen, S. E., & Manning, C. E. (1999). Geological implications of a permeability-depth curve for the continental crust. *Geology*, *27*(12), 1107–1110. https://doi.org/10.1130/0091-7613(1999)027%3C1107:GIOAPD%3E2.3.CO;2

Leibowitz, S. G., Comeleo, R. L., Wigington, P. J., Weber, M. H., Sproles, E. A., & Sawicz, K. A. (2016). Hydrologic landscape characterization for the Pacific Northwest, USA. *JAWRA Journal of the American Water Resources Association*, *52*(2), 473–493.

Maxwell, R. M., & Condon, L. E. (2016). Connections between groundwater flow and transpiration partitioning. *Science*, *353*(6297), 377–380. https://doi.org/10.1126/science.aaf7891

Maxwell, R. M., Condon, L. E., & Kollet, S. J. (2015). A high-resolution simulation of groundwater and surface water over most of the continental US with the integrated hydrologic model ParFlow v3. *Geoscientific Model Development*, *8*(3), 923–937.

Maxwell, R. M., Condon, L. E., Kollet, S. J., Maher, K., Haggerty, R., & Forrester, M. M. (2016). The imprint of climate and geology on the residence times of groundwater. *Geophysical Research Letters*, *43*(2), 701–708. https://doi.org/10.1002/2015GL066916

Milly, P. C. D., Malyshev, S. L., Shevliakova, E., Dunne, K. A., Findell, K. L., Gleeson, T., et al. (2014). An enhanced model of land water and energy for global hydrologic and Earth-system studies. *Journal of Hydrometeorology*, *15*(5), 1739–1761.

Shangguan, W., Hengl, T., Mendes de Jesus, J., Yuan, H., & Dai, Y. (2017). Mapping the global depth to bedrock for land surface modeling. *Journal of Advances in Modeling Earth Systems*, *9*, 65–88. https://doi.org/10.1002/2016MS000686

Sutanudjaja, E. H., van Beek, L. P. H., de Jong, S. M., van Geer, F. C., & Bierkens, M. F. P. (2014). Calibrating a large-extent high-resolution coupled groundwater-land surface model using soil moisture and discharge data. *Water Resources Research*, *50*, 687–705. https://doi.org/10.1002/2013WR013807

Xu, X., & Liu, W. (2017). The global distribution of Earth's critical zone and its controlling factors. *Geophysical Research Letters*, *44*, 3201–3208. https://doi.org/10.1002/2017GL072760